Effects of graphene on electro-optic response and ion-transport in a nematic liquid crystal

Rajratan Basu,[a] Alfred Garvey, and Daniel Kinnamon
Department of Physics, Soft Matter and Nanomaterials Laboratory, The United States Naval Academy, Annapolis, Maryland 21402, USA

(Received 22 November 2014; accepted 6 February 2015; published online 17 February 2015)

A small quantity of graphene, containing both monolayer and multilayer flakes, was doped in a nematic liquid crystal (LC), and the nematic electro-optic switching was found to be significantly faster in the LC + graphene hybrid than that of the pure LC. Additional studies revealed that the presence of graphene reduced the free ion concentration in the nematic media by ion-trapping process. The reduction of mobile ions in the LC was found to have subsequent impacts on the LC's conductivity and rotational viscosity, allowing the nematic director to respond quicker on switching the electric field on and off. © *2015 AIP Publishing LLC*. [http://dx.doi.org/10.1063/1.4908608]

I. INTRODUCTION

Nematic liquid crystals (LCs) are technologically important materials for their applications in electro-optical display technology. Therefore, studying the electro-optic response of nematic LCs is an active research area in both fundamental and applied physics.[1,2] In a different direction, LCs and their multifaceted interactions with various nanomaterials have been an intriguing topic of research area over the past decade. For examples, the nematic phase can transfer its long-range orientational order onto various nanoparticles;[3–7] the presence of carbon nanotubes can enhance the LC's electro-optical responses;[8,9] chiral carbon nanotubes can transmit their surface chirality into otherwise achiral LCs through π–π stacking;[10–13] quantum dots can be self-assembled in the nematic matrix;[14–16] and ferroelectric nanoparticles can significantly enhance the LC's orientational order parameter and electro-optical response, reducing the orientational threshold voltage.[17–28]

Graphene is a crystalline allotrope of carbon with 2-dimensional properties. The carbon atoms in a graphene sheet are densely packed in a regular sp^2-bonded atomic-scale hexagonal pattern. This 2-dimensional honeycomb structure of graphene makes it an interesting and important nanomaterial to study the LC—nanomaterial interactions along a new direction. For examples, transparent graphene-conducting-layers can be used as electrodes to produce high-transmittance liquid crystal displays;[29,30] the honeycomb graphene surface can be used to enhance the spontaneous polarization of a ferroelectric liquid crystal;[31] the vertical alignment of LC molecules can be achieved by graphene-oxide without any surface treatment of the substrate;[32] graphene with benzene can enhance the orientational order in a nematic phase;[33] and functionalized graphene can mutually self-assemble discotic liquid crystals.[34]

In this paper, we experimentally demonstrate that the presence of a dilute concentration of graphene flakes in a nematic LC significantly accelerates the electro-optic response of the nematic switching. The presence of graphene also decreases ion-transport in the LC, which results in a reduction of rotation viscosity in the mixture.

II. EXPERIMENTS AND RESULTS

The graphene sample, obtained from Nanostructured and Amorphous Materials, Inc., contained both monolayer and multilayer flakes of thickness ranging from 0.55 nm to 3.74 nm. The flakes were circular in shape and had an average diameter of 1.75 μm (minimum diameter = 0.5 μm and maximum diameter = 3.0 μm). A small amount of graphene sample was first dispersed in toluene and mixed by a micro-homogenizer tip of 5 mm diameter at 35 000 rpm for 3 h, followed by sonication for 5 h. The liquid crystal 4-cyano-4′-pentylbiphenyl (5CB; nematic to isotropic transition at $T_{NI} = 36.0\,^{\circ}C$) then was added to the toluene + graphene mixture and sonicated for 5 h, allowing the LC to dissolve completely into the solution. Finally, the toluene was evaporated at an elevated temperature, leaving a pure LC + graphene mixture of 0.005 wt. %. For consistency, the pure LC was also treated the same way, such as dissolving in toluene followed by a slow evaporation and degassing. Commercially manufactured LC cells (SA100A200uG180, planar rubbed from Instec, Inc.) with a 1.5° pre-tilt angle, 1 cm^2 semitransparent indium tin oxide (ITO) coated area, and a $d = 20 \pm 0.15$ μm spacing were used for our experiments. Two cells were filled at temperature $T > 46\,^{\circ}C$ in the isotropic phase by capillary action, one with LC only and the other with the LC + graphene mixture. Note that the cell spacing tends to filter out any aggregates larger than d. Before performing any measurements, the graphene-doped LC cell was examined using a polarizing optical microscope. The optical micrographs revealed uniform nematic textures, like that of the pure LC cell, indicating a uniform *director field* (average direction of LC molecules). There was no indication of phase separation or agglomerates at any temperature. See the optical micrographs in the inset in Figure 1(a) [(i) and (ii) represent the textures for the pure LC and the LC + graphene mixture, respectively]. Thus, at least on the

[a]Electronic mail: basu@usna.edu

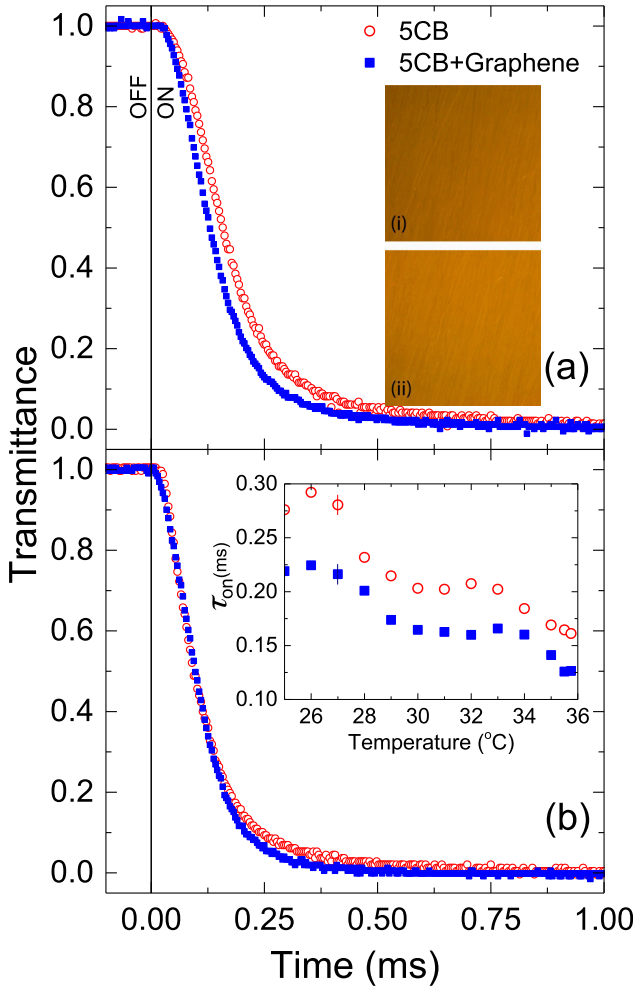

FIG. 1. Normalized transmittance as function of time for 5CB and 5CB + graphene at (a) 25 °C and (b) 33 °C after the voltage (30 V) is turned ON at $t = 0$. Inset in (a): nematic textures for (i) 5CB and (ii) 5CB + graphene under a crossed polarized microscope. Inset in (b): τ_{on} as a function of temperature for 5CB and 5CB + graphene.

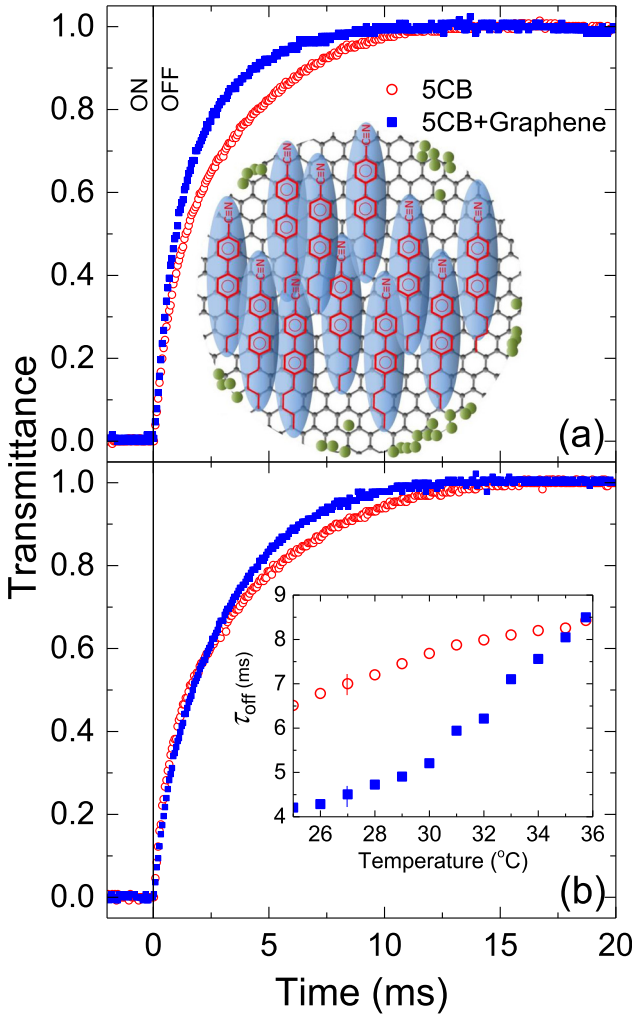

FIG. 2. Normalized transmittance as function of time for 5CB and 5CB + graphene at (a) 25 °C and (b) 33 °C after the voltage (30 V) is turned OFF at $t = 0$. Inset in (a): A schematic illustration of the π–π stacking between a graphene surface (black honeycomb structure) and 5CB LC (red molecules); it also illustrates how ions (green spheres) are trapped by the graphene flake. Inset in (b): τ_{off} as a function of temperature for 5CB and 5CB + graphene.

length scales resolvable by visible light, the structure of graphene-aggregates (if any) must be small enough that they do not significantly perturb the director field due to their low concentration and uniform dispersion.

The field-induced nematic switching was studied from the electro-optic response of the LC cells. The optical setup consisted of a beam from a 5-mW He-Ne laser at wavelength 633 nm that passed through a polarizer, the cell, a crossed analyzer and into a nanosecond Newport detector. The beam was polarized at an angle of 45° with respect to the cell's rubbing direction. The output of the detector was fed into a digital storage oscilloscope. A dc voltage pulse of 30 V (much higher than the threshold switching voltage) at a pulse interval of 25 Hz was applied across the cell and, the change in transmittance intensity as a function of time (both when the voltage was turned on and off) was detected by the oscilloscope. Transmittance responses for field on and off were studied as a function of temperature for pure 5CB and 5CB + grapheme samples. The setup was computer controlled and data acquisition was performed using LabVIEW® software.

Figures 1 and 2 represent the normalized transmittance intensity responses as a function of time for voltage on and off, respectively. Figures 1(a) and 1(b) depict that when the applied voltage is turned on, the transmittance intensity drops as a function of time for 5CB and 5CB + graphene at two different temperatures. It is clear from Figure 1 that 5CB + graphene sample responses were faster than pure 5CB. The time the transmittance intensity takes to drop from 90% to 10% of the maximum intensity, after the voltage is turned on, is defined as the optical switching on, τ_{on}. The inset in Figure 1(b) shows τ_{on} as a function of temperature for 5CB and 5CB + graphene. This inset manifests that τ_{on} always stays faster for the LC + graphene hybrid in the temperature range studied. Figures 2(a) and 2(b) illustrate that when the applied voltage is turned off, the transmittance intensity increases as a function of time for 5CB and 5CB + graphene at two different temperatures. Like Figure 1, it is apparent from Figure 2 that 5CB + graphene relaxes faster than pure 5CB when the voltage is turned off. The time the transmittance intensity takes to rise from 10% to 90% of the maximum intensity, after the voltage is turned off, is defined as the optical switching off, τ_{off}. The inset in Figure 2(b) shows

τ_{off} as a function of temperature for 5CB and 5CB + graphene. This inset also exhibits that τ_{off} is faster for the LC + graphene hybrid than that of the pure LC in the temperature range studied.

The two characteristic times,[35] rise (voltage on) and decay (voltage off), of the director can be described as

$$\tau_{rise} = \frac{\gamma_1 d^2}{\Delta\varepsilon\,\varepsilon_o V^2 - K_{11}\pi^2}, \quad \tau_{decay} = \frac{\gamma_1 d^2}{K_{11}\pi^2}, \tag{1}$$

where γ_1 is the rotational viscosity, d is the cell thickness, $\Delta\varepsilon$ is the dielectric anisotropy, ε_0 the is free space permittivity, K_{11} is the splay elastic constant, and V is the applied voltage. Note that τ_{rise} and τ_{decay} are not equal to the electro-optical responses, τ_{on} and τ_{off}, respectively. τ_{rise} is the time the nematic director takes to rotate from planar to homeotropic configuration, when the voltage is turned on. And similarly, τ_{decay} is the time the director takes to rotate back from homeotropic to planar configuration after the voltage is turned off. The optical response is mainly due to the director's rotation after the field is turned on or off. Therefore, neglecting the backflow in the cell, one can write $\tau_{rise} \propto \tau_{on}$ and $\tau_{decay} \propto \tau_{off}$. From Eq. (1), for a constant d and V, the director's response would be faster for a reduced γ_1, an enhanced $\Delta\varepsilon$, and a reduced K_{11}.

Our measurements show that a 0.005 wt. % of graphene sample does not alter $\Delta\varepsilon$ and K_{11} of 5CB significantly. We therefore performed experiments to study γ_1 of the samples. The rotational viscosity for the nematic samples was obtained by measuring the transient current induced by a dc voltage across a planar-aligned configuration.[36,37] When a dc voltage (much higher than the threshold voltage) is applied across a planar LC cell, the induced current $I(t)$ through the cell shows a time response as the director goes through the dynamic rotation. The current response is given by

$$I(t) = \frac{A\,(\Delta\varepsilon\,\varepsilon_o)^2\,E^3}{\gamma_1}\sin^2[2\varphi(t)], \tag{2}$$

where A is the area of the cell, E $(=V/d)$ is the electric field, and φ is the angle the director makes with the electrodes/substrate at a given time. At $\varphi = 45°$, $I(t)$ reaches its peak $I_p = \frac{A\,(\Delta\varepsilon\,\varepsilon_o)^2\,E^3}{\gamma_1}$ at the peak time,

$$t_p = \left[\frac{\gamma_1\left(-\ln(\tan\varphi_o)\right)}{\Delta\varepsilon\varepsilon_o}\right]\frac{1}{E^2}, \tag{3}$$

where φ_o is the pre-tilt angle. Note, $\varphi_o = 1.5°$ for the cells used in this experiment. A dc voltage pulse of 25 V with a pulse interval of 1 Hz was applied across the cell to generate $I(t)$. Then, $I(t)$ in the cell was detected as a function of time through a load resistor in series by a digital storage oscilloscope. The peak time, t_p, was detected from $I(t)$ to extract γ_1 from the known values of E and $\Delta\varepsilon$. Figure 3 represents γ_1 as a function of temperature for pure 5CB and 5CB + graphene hybrid. The inset in Figure 3 shows $I(t)$, induced by a 25 V applied voltage, as a function of time for 5CB + graphene hybrid at three different temperatures. Figure 3 depicts that the rotation viscosity of the hybrid has a lower rotation

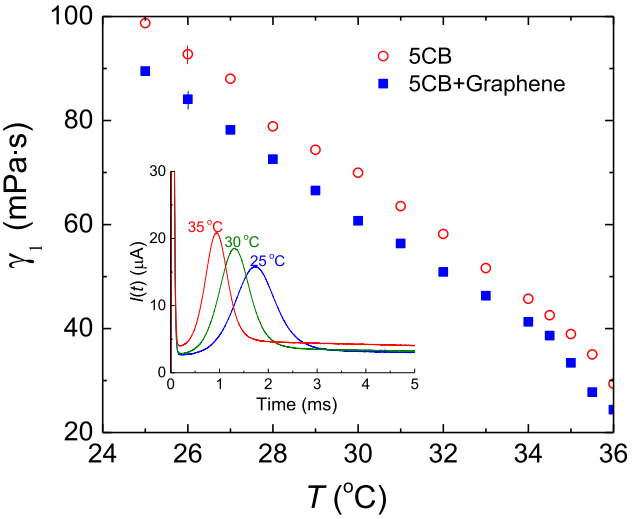

FIG. 3. Rotational viscosity, γ_1 for 5CB and 5CB + graphene as a function of temperature. Typical error bars are shown. Inset: Transient current, $I(t)$ as a function of time for 5CB + graphene at three different temperatures.

viscosity than that of the pure LC. The rotational viscosity of an aligned liquid crystal represents an internal friction among LC directors during the rotation process. The magnitude of γ_1 depends on the structure of detailed molecular constituents, intermolecular association, temperature, and the presence of ions. Since the low concentration of graphene does not alter $\Delta\varepsilon$ and K_{11} of 5CB significantly, it is presumed that the intermolecular association in 5CB does not change significantly. There are several reports in the literature that show the presence of fewer ions can decrease the rotation viscosity of an LC.[25,26,31,38] We therefore have carried out experiments to study the ion-transport in the LC samples as a function of temperature.

The presence of free ions in the pure LC and LC + graphene hybrid was measured by detecting the ion-bump[39] of a transient current generated by inverting the voltage at opposite electrodes in the LC cell. The nematic phase of an LC shows dielectric anisotropy $\Delta\varepsilon$ due to the anisotropic nature of the molecules. For a positive dielectric anisotropic LC, like 5CB, the director field reorients parallel to an applied electric field. In a uniform homogeneously aligned parallel-plate cell configuration, the nematic director is initially aligned perpendicular to the applied electric field E due to the LC-substrate surface anchoring; but when the field magnitude is above a critical threshold, the director can reorient parallel to the applied field, obtaining a homeotropic configuration. This orientation process occurs because the nematic system is dielectrically anisotropic and experiences a torque proportional to $\Delta\varepsilon\,E^2$ (Ref. 40) in an external electric field. The orientation process depends on the *magnitude* of the field and not on its *sign*. So, when a constant square wave is applied across a nematic LC cell (i.e., the voltage is inverted at opposite electrodes), the LC molecules do not rotate. However, positive and negative ions in the LC cell, that are initially separated at the two electrodes, start to move towards the opposite electrodes after the voltage is inverted, causing an ion current, I_{ion} in the cell. When the positive and negative ions meet at $d/2$ (i.e., at the middle of the cell), I_{ion}

reaches its peak value at peak time, $t_{ion-peak} = \frac{d^2}{2\mu E}$, where μ is the mobility.[39] Finally I_{ion} drops to zero when the positive ions reach the negative electrode and the negative ions reach the positive electrode of the cell. The total ion transport in the cell then can be calculated by taking the area under the I_{ion} vs. time curve. A square wave of 18 V at 1 Hz was applied using an Automatic Liquid Crystal Tester (Instec, Inc.) to detect I_{ion} for the pure LC and LC + graphene hybrid. The ion concentration n_i (C/m^3) was extracted using the cell's known dimension.

Figure 4(a) shows the ion concentration, n_i as a function of temperature in the nematic phase for 5CB and 5CB + graphene. The inset in Figure 4(a) shows the time dependent ion current, I_{ion} for 5CB and 5CB + graphene mixture. Note that we have used the same type of commercially available cells from Instec, Inc for all measurements. Therefore, if there are any ions generated from the cell's polymer alignment layers and/or the surrounding glue, they must be consistent in both the cells, and thus, the observed change in n_i is only due to the presence of graphene. Figure 4(a) clearly depicts that the ion transport is greatly reduced when graphene is doped in 5CB. Note that n_i increases with increasing temperature because of more ion-transport at higher temperature.

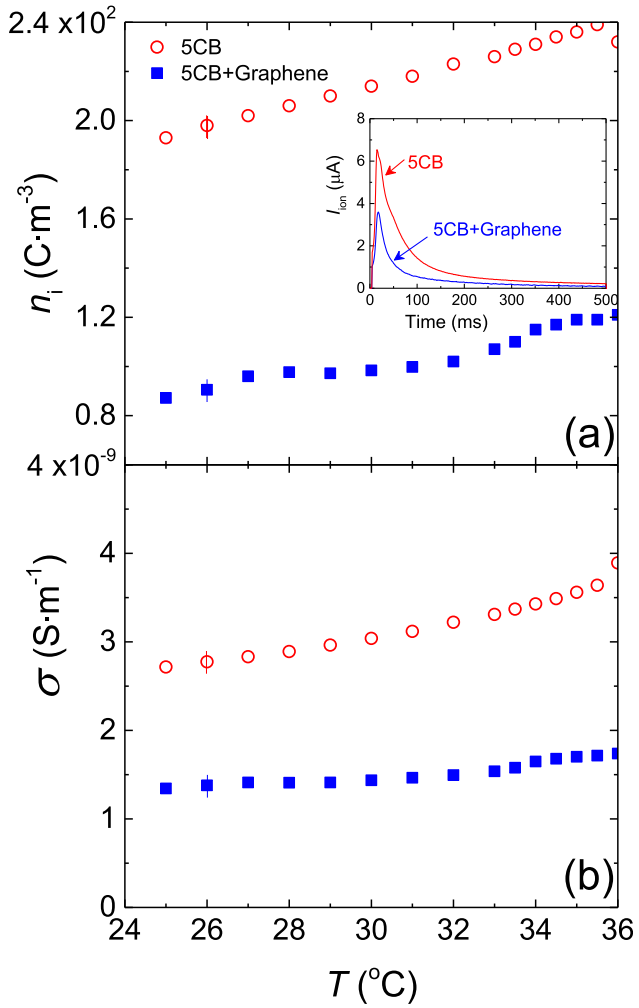

FIG. 4. Free ion concentration, n_i as a function of temperature for 5CB and 5CB + graphene. Typical error bars are shown. Inset: Ion current, I_{ion} as a function of time for 5CB and 5CB + graphene at 26 °C after the voltage is inverted across the cells. The peak represents the ion-bump when positive and negative ions meet at the middle of the cell. (b) Conductivity, σ as a function of temperature for 5CB and 5CB + graphene mixtures listed in the legend.

III. DISCUSSIONS

To reduce the elastic distortion in a nematic matrix, graphene flakes align themselves in such a way that the plane of the sheet is parallel to the nematic director,[41] employing the π–π electron stacking between the honeycomb structure of graphene and benzene rings of the LC. Graphene acts a conductor to electric fields in the plane of the graphene sheets and as an insulator to perpendicular electric fields. So in a planar aligned cell the graphene flakes do not significantly contribute to the electrical conductivity of the cell. The electrical conductivity, σ of the LC is therefore proportional to the ion concentration in the LC. Thus, measuring σ is another reliable way of measuring the ionic content in a solution.[42] Figure 4(b) illustrates σ as a function of temperature in the nematic phase for pure 5CB and 5CB + graphene mixture. Clearly, the presence of graphene reduces the conductivity, revealing the presence of fewer mobile ions in 5CB + graphene hybrid.

It has been recently shown that a finite graphene sheet (diameter $<1\,\mu$m) has a nonzero electrostatic field near the surface.[43] The electrostatic field decays only slowly with increasing size and is always non-negligible near edges.[43] In our experiments, the diameter of the graphene flakes has a range from 0.5 μm to 3.0 μm. Therefore, the electrostatic fields from these finite graphene sheets, mainly from those that are below 1 μm, can capture some of the mobile ions in the LC media. The larger sheets can also trap some free ions on their edges due to the presence of non-vanishing electrostatic fields. Even without the electrostatic fields, it is possible that the multilayer graphene flakes act as *screens* where some of the ions get trapped when they move from one electrode to the other. Both the processes reduce the free ion concentration in the LC. The presence of fewer ions reduces the internal friction (and hence γ_1 of the LC media), allowing the LC molecules to rotate faster. At this point, we can state that the measured reduction in ion-concentration is not linearly proportional to the reduction in γ_1 in the LC + graphene system. Note that the graphene flakes themselves act as external additives in the LC, and can increase the internal friction. Therefore, in one direction, the reduction of free ions tends to decrease γ_1 and in another direction, the flakes tend to increase γ_1. Since the concentration of the graphene flakes is very small, their presence cannot overmatch the effect of the reduction of ions on γ_1. Therefore, a quantitative argument on the relation between the ion-reduction and γ_1 in this complex system would be difficult to make.

The anchoring energy has a significant effect on the decay time, τ_{decay}. The anchoring energy is related to τ_{decay} as $\tau_{decay} \propto \frac{\gamma_1 d}{W}$,[1,44,45] where W is the anchoring strength coefficient. It has been shown in the literature that when carbon nanotubes (similar to graphene's honeycomb structure) are doped in an LC the anchoring energy of the composite is significantly enhanced[46–48] due to the π–π anchoring. Thus, it is also expected that the presence of graphene in the nematic

LC would result in an increase in anchoring energy due to the same π–π electron stacking between the LC molecules, the graphene flakes, and the alignment layers. The above relation between τ_{decay} and W indicates that an increase in anchoring energy should lower the response time—which is consistent with our findings, as reflected in Figs. 1 and 2.

IV. CONCLUSIONS

We have experimentally demonstrated that when a small quantity of monolayer and multilayer combination of graphene flakes is dispersed in 5CB LC, the electro-optic response of the nematic switching gets faster. In addition, the dispersed graphene flakes reduce the ion-transport by sweeping some concentration of mobile ions—which may have potential applications in LC based electro-optic devices. In liquid crystal displays, the presence of excess ions causes several problems, such as slow responses, long-term image sticking effects, and short-term flicker effects.[49–54] Understanding the ion-transport phenomenon in an LC and the principles governing their subsequent effects on the LC's electrical and electro-optical properties is active area of research.[55–62] Therefore, the results presented in this paper are important for developing novel methods of purifying LCs from excess ions without additional chemical synthesis. Our studies motivate various important questions and subsequent experiments are planned for the future to address several issues, such as understanding the separate effects of monolayer and multilayer flakes, with their different sizes, on the LC's ion-transport, rotational viscosity, and electro-optic effects.

ACKNOWLEDGMENTS

This work was supported by the Office of Naval Research (Division 312: Electronics Sensors and Network Research) under Award No. N0001414WX20791.

[1]L. M. Blinov and V. G. Chigrinov, *Electro-optic Effects in Liquid Crystal Materials* (Springer-Verlag, New York, 1996).
[2]V. Borshch, S. V. Shiyanovskii, and O. D. Lavrentovich, Phys. Rev. Lett. **111**, 107802 (2013).
[3]M. D. Lynch and D. L. Patrick, Nano Lett. **2**, 1197 (2002).
[4]I. Dierking, G. Scalia, and P. Morales, J. Appl. Phys. **97**, 044309 (2005).
[5]R. Basu and G. Iannacchione, Appl. Phys. Lett. **93**, 183105 (2008).
[6]I.-S. Baik, S. Y. Jeon, S. H. Lee, K. A. Park, S. H. Jeong, K. H. An, and Y. H. Lee, Appl. Phys. Lett. **87**, 263110 (2005).
[7]R. Basu and G. S. Iannacchione, Phys. Rev. E **80**, 010701 (2009).
[8]H.-Y. Chen, W. Lee, and N. A. Clark, Appl. Phys. Lett. **90**, 033510 (2007).
[9]R. Basu, Appl. Phys. Lett. **103**, 241906 (2013).
[10]R. Basu, K. A. Boccuzzi, S. Ferjani, and C. Rosenblatt, Appl. Phys. Lett. **97**, 121908 (2010).
[11]R. Basu, R. G. Petschek, and C. Rosenblatt, Phys. Rev. E **83**, 041707 (2011).
[12]R. Basu, C.-L. Chen, and C. Rosenblatt, J. Appl. Phys. **109**, 083518 (2011).
[13]R. Basu, C. Rosenblatt, and R. Lemieux, Liq. Cryst. **39**, 199 (2012).
[14]A. L. Rodarte, R. J. Pandolfi, S. Ghosh, and L. S. Hirst, J. Mater. Chem. C **1**, 5527 (2013).
[15]A. L. Rodarte, C. Gray, L. S. Hirst, and S. Ghosh, Phys. Rev. B **85**, 035430 (2012).
[16]J. Mirzaei, M. Reznikov, and T. Hegmann, J. Mater. Chem. **22**, 22350 (2012).
[17]A. N. Morozovska, M. D. Glinchuk, and E. A. Eliseev, Phys. Rev. B **76**, 014102 (2007).
[18]M. Copic, A. Mertelj, O. Buchnev, and Y. Reznikov, Phys. Rev. E **76**, 011702 (2007).
[19]L. M. Lopatina and J. V. Selinger, Phys. Rev. Lett. **102**, 197802 (2009).
[20]F. Li, O. Buchnev, C. Il Cheon, A. Glushchenko, V. Reshetnyak, Y. Reznikov, T. J. Sluckin, and J. L. West, Phys. Rev. Lett. **97**, 147801 (2006).
[21]Y. Reznikov, O. Buchnev, O. Tereshchenko, V. Reshetnyak, A. Glushchenko, and J. West, Appl. Phys. Lett. **82**, 1917 (2003).
[22]Y.-S. Ha, H.-J. Kim, H.-G. Park, and D.-S. Seo, Opt. Express **20**, 6448 (2012).
[23]J.-F. Blach, S. Saitzek, C. Legrand, L. Dupont, J.-F. Henninot, and M. Warenghem, J. Appl. Phys. **107**, 074102 (2010).
[24]A. Rudzki, D. R. Evans, G. Cook, and W. Haase, Appl. Opt. **52**, E6 (2013).
[25]S. A. Basun, G. Cook, V. Yu. Reshetnyak, A. V. Glushchenko, and D. R. Evans, Phys. Rev. B **84**, 024105 (2011).
[26]M. R. Herrington, O. Buchnev, M. Kaczmarek, and I. Nandhakumar, Mol. Cryst. Liq. Cryst. **527**, 72/[228] (2010).
[27]R. Basu, Phys. Rev. E **89**, 022508 (2014).
[28]A. Mikulko, P. Arora, A. Glushchenko, A. Lapanik, and W. Haase, Europhys. Lett. **87**, 27009 (2009).
[29]P. Blake, P. D. Brimicombe, R. R. Nair, T. J. Booth, D. Jiang, F. Schedin, L. A. Ponomarenko, S. V. Morozov, H. F. Gleeson, E. W. Hill, A. K. Geim, and K. S. Novoselov, Nano Lett. **8**, 1704 (2008).
[30]Y. U. Junga, K. W. Parka, S. T. Hura, S. W. Choia, and S. J. Kanga, Liq. Cryst. **41**, 101 (2014).
[31]R. Basu, Appl. Phys. Lett. **105**, 112905 (2014).
[32]A. Malik, A. Choudhary, P. Silotia, A. M. Biradar, V. K. Singh, and N. Kumar, J. Appl. Phys. **108**, 124110 (2010).
[33]T. M. Alam and C. J. Pearce, Chem. Phys. Lett. **592**, 7 (2014).
[34]A. B. Shivanandareddy, S. Krishnamurthy, V. Lakshminarayanan, and S. Kumar, Chem. Commun. **50**, 710 (2014).
[35]E. Jakeman and E. P. Raynes, Phys. Lett. **39A**, 69 (1972).
[36]M. Imai, H. Naito, M. Okuda, and A. Sugimura, Jpn. J. Appl. Phys., Part 1 **33**, 3482 (1994).
[37]M. Imai, H. Naito, M. Okuda, and A. Sugimura, Mol. Cryst. Liq. Cryst. Sci. Technol., Sect. A **259**, 37 (1995).
[38]R. Basu and A. Garvey, Appl. Phys. Lett. **105**, 151905 (2014).
[39]Z. Zou, N. A. Clark, and M. A. Handschy, Ferroelectrics **121**, 147 (1991).
[40]P. G. De Gennes and J. Prost, *The Physics of Liquid Crystals* (Oxford University Press, New York, 1994).
[41]D. W. Kim, Y. H. Kim, H. S. Jeong, and H.-T. Jung, Nat. Nanotechnol. **7**, 29 (2012).
[42]J. O'M. Bockris and A. K. N. Reddy, *Modern Electrochemistry 1: Ionics*, 2nd ed. (Kluwer Academic Publishers, New York, 2000).
[43]M. Kocman, M. Pykal, and P. Jurecka, Phys. Chem. Chem. Phys. **16**, 3144 (2014).
[44]X. Nie, R. Lu, H. Xianyu, T. X. Wu, and S. T. Wu, J. Appl. Phys. **101**, 103110 (2007).
[45]S. V. Pasechnik, V. G. Chigrinov, and D. V. Shmeliova, *Liquid Crystals: Viscous and Elastic Properties* (Wiley-VCH, Weinheim, Germany, 1999).
[46]K. A. Park, S. M. Lee, S. H. Lee, and Y. H. Lee, J. Phys. Chem. C **111**, 1620 (2007).
[47]S. Y. Lu and L. C. Chien, Opt. Express **16**, 12777 (2008).
[48]S. Y. Jeon, K. A. Park, I. S. Baik, S. J. Jeong, S. H. Jeong, K. H. An, S. H. Lee, and Y. H. Lee, Nano **2**, 41 (2007).
[49]S. Takahashi, J. Appl. Phys. **70**, 5346 (1991).
[50]H. De Vleeschouwer, B. Verweire, K. D'Have, and H. Zhang, Mol. Cryst. Liq. Cryst. **331**, 567 (1999).
[51]H. De Vleeschouwer, F. Bougrioua, and H. Pauwels, Mol. Cryst. Liq. Cryst. **360**, 29 (2001).
[52]H. De Vleeschouwer, A. Verschueren, F. Bougrioua, R. van Asselt, E. Alexander, S. Vermael, K. Neyts, and H. Pauwels, Jpn. J. Appl. Phys., Part 1 **40**, 3272 (2001).
[53]K. H. Yang, J. Appl. Phys. **67**, 36 (1990).
[54]N. Sasaki, Mol. Cryst. Liq. Cryst. **367**, 671 (2001).
[55]K. Neyts, S. Vermael, C. Desimpel, G. Stojmenovik, R. van Asselt, A. R. M. Verschueren, D. K. G. de Boer, R. Snijkers, P. Machiels, and A. van Brandenburg, J. Appl. Phys. **94**, 3891 (2003).
[56]M. Yamashita and Y. Amemiya, Jpn. J. Appl. Phys. **17**, 1513 (1978).
[57]V. Novotny, J. Appl. Phys. **50**, 2787 (1979).
[58]A. Sugimura, N. Matsui, Y. Takahashi, H. Sonomura, H. Naito, and M. Okuda, Phys. Rev. B **43**, 8272 (1991).
[59]H. Naito, M. Okuda, and A. Sugimura, Phys. Rev. A **44**, R3434 (1991).
[60]H. Naito, K. Yoshida, and M. Okuda, J. Appl. Phys. **73**, 1119 (1993).
[61]C. Colpaert, B. Maximus, and A. De Meyere, Liq. Cryst. **21**, 133 (1996).
[62]A. Sawada, A. Manabe, and S. Nameura, Jpn. J. Appl. Phys., Part 1 **40**, 220 (2001).